Impact of Data Acquisition System on Impedance-based Fault Locators

P. V. B. Oliveira, W. L. A. Neves, D. Fernandes Jr., R. L. A. Reis

***Abstract*—In this paper, the impact of the data acquisition system on the performance of one- and two-ended impedance-based fault location techniques is evaluated. Basically, one CCVT, one anti-aliasing filter, and three ADC converter are taken into account. Several fault simulations were performed in the Alternative Transients Program (ATP), varying the fault type, location, resistance and incipient angle. In each case, the fault point was estimated considering as input data the signals from the primary, secondary, filtered secondary, and the signals sampled by the ADC. From the obtained results, it is verified that the estimated fault locations are directly affected by the CCVT and anti-aliasing filter transient responses, and the error introduced by the ADC.**

***Keywords*—Fault location, impedance-based, data acquisition system, power system protection, electromagnetic transients.**

I. Introduction

THE power system protection is of great importance due to its inherent functions of protecting the power network and ensure service continuity. Basically, it can be defined as a set of equipment with the purpose of protecting the power system against faults and any other abnormal operating conditions [2]. It is therefore necessary to carry out a close monitoring of the electrical quantities to guarantee reliable measurements and a precise performance of protection systems.

The voltage and current signals coming from power systems are transmitted to protection and control systems via instrument transformers (IT), such as coupling capacitor voltage transformer (CCVT) and Current Transformers (CT), in order to obtain information about the power system which they are connected to. During steady-state, the IT secondary voltage and current waveforms are almost ideal replica of the primary signal at fundamental frequency. However, when a fault occurs on the transmission line (TL), undesirable wave shapes may appear in the secondary signals of IT due to their electromagnetic coupling design, which may lead to malfunctioning or delay in the tripping process of protective devices and fault locators [1].

This work was supported by the Brazilian Coordination for the Improvement of Higher Education Personnel (CAPES).

P. V. B. Oliveira is with the Department of Electrical Engineering of Federal University of Campina Grande (UFCG), 58429-900 Campina Grande, Paraiba, Brazil (email: paulo.oliveira@ee.ufcg.eud.br).

W. L. A. Neves and D. Fernandes Jr. are with the Department of Electrical Engineering of Federal University of Campina Grande (UFCG) (email: waneves@dee.ufcg.edu.br and damasio@dee.ufcg.edu.br).

R. L. A. Reis is with Federal Rural University of Pernambuco, 52.171-011 Cabo de Santo Agostinho, Brazil, and currently he is a PhD student at Federal University of Campina Grande (UFCG), Campina Grande, Brazil (email: raphael.reis@ufrpe.br).

Paper submitted to the International Conference on Power Systems Transients (IPST2019) in Perpignan, France June 17-20, 2019.

Impedance-based fault location techniques extract fundamental frequency information from the data acquisition system of numerical relays or fault locators to compute the apparent impedance. In this way, before the IT secondary signals are sampled by an analog-to-digital converter (ADC) to be processed by protection algorithms, analog anti-aliasing filters are used to limit the signal bandpass and avoid frequency and phase changes on the sampled signals (aliasing phenomenon) [1]. Second and third order Butterworth, Chebyshev, and Bessel filters are usually used in protection application [2].

After the filtering process, voltage and current signals are sampled by ADC, which converts an analog signal into a digital word of several bits. Analog signals can assume an infinite amount of values within a certain interval but digital ones can assume only a finite quantity of values within the same interval. Thus, it is necessary to perform a quantization or rounding of the sampled signal before this information can be converted into a binary word [3]. This process may also introduce errors that can affect the performance of fault location methods.

In the literature, there are several references indicating the impact of parts of the data acquisition system on the performance of protection [4], [5] and fault locator algorithms [1], [6], [7], [8]. However, analyses concerning the influence of ADC in cascade with IT and anti-aliasing filters on fault locators are still scarce in the literature, which demands more investigations.

The aim of the current work is to carry out a thorough investigation about the influence of the complete data acquisition system. In this way, the impact of a 230 kV CCVT, reported in the literature, one anti-aliasing filter, and three ADC with different word sizes on an one- and two-ended impedance-based fault location techniques is analyzed. The evaluations are performed through several short-circuit simulations using the Alternative Transients Program (ATP) [9]. In each simulation, the fault variables were varied (fault type, location, resistance, and inception angle) and the relative errors were estimated considering signals from the power system primary side (taken as reference here), secondary signals, filtered secondary signals, and sampled signals (considering all parts of the data acquisition system) as input data to the routines.

II. The Analyzed Data Acquisition System

A simplified diagram of a data acquisition system used in protection applications is shown in Fig. 1. In this system, the current and voltage are measured by the a CT and a

CCVT, respectively, and then filtered by the anti-aliasing filter and sampled by the ADC prior to be used as input data in protection applications.

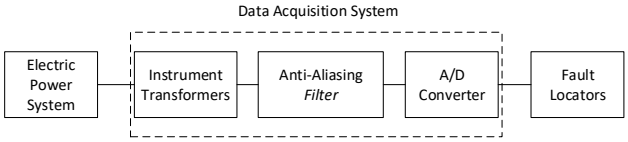

Fig. 1: Simplified diagram of a data acquisition system.

A. The Analyzed CCVT

The CCVTs are widely used in high voltage systems to provide scaled-down voltage measurements to protection and control devices [4]. In this paper, the transient behavior of one 230 kV CCVT is evaluated. The required circuit topology and data parameters are shown in Fig. 2 and Table I, respectively.

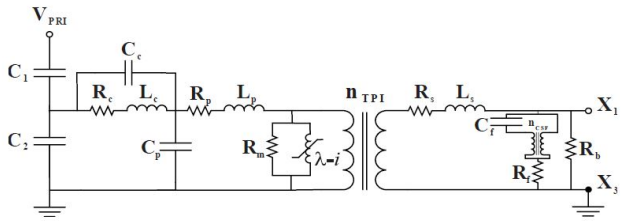

Fig. 2: The CCVT's circuit topology [10].

TABLE I: The CCVT's parameters

Parameter	Value
$C_1(nF)$	2.43
$C_2(nF)$	82
$C_c(pF)$	100
$C_p(pF)$	150
$C_f(\mu F)$	9.6
$L_c(H)$	153.85
$L_p(H)$	7.95
$L_s(\mu H)$	2.653
$R_c(\Omega)$	228
$R_p(\Omega)$	400
$R_s(\Omega)$	0.001
$R_f(\Omega)$	40
$R_b(\Omega)$	100
n_{CSF}	1.98
$n_{TPI}(X_1\text{-}X_3)$	57.25
$\lambda(V.s)$	13.7867
$i(mA)$	1.421

The CCVT frequency response was obtained using the ATP Frequency Scan routine [9] with a range of 10 Hz to 10 kHz. The CCVT magnitude and phase frequency responses are shown in Figs. 3(a) and 3(b), respectively . In order to make possible to compare the primary voltage (considered as reference in this paper) with the secondary voltage, the voltage magnitude frequency responses were normalized in per unit values and the phase responses in degrees.

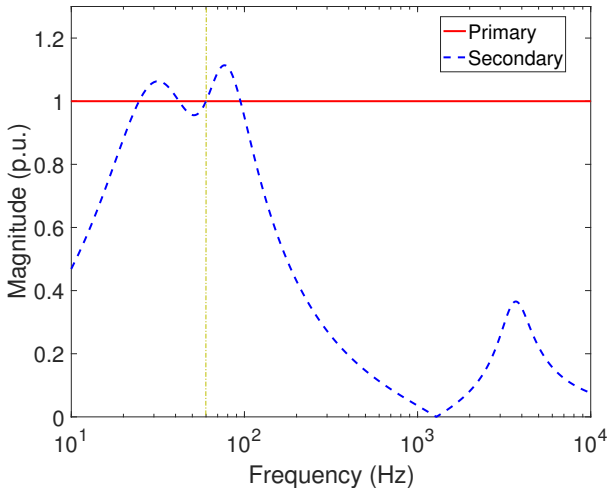

(a)

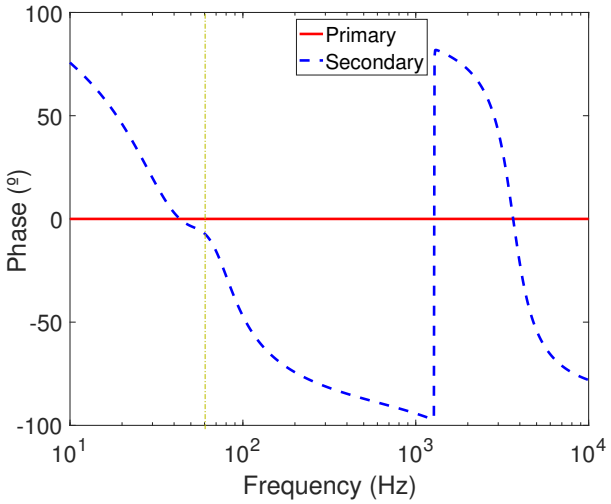

(b)

Fig. 3: CCVT frequency response: (a) Magnitude (p.u.); (b) Phase (°).

From Fig. 3, it can be seen that at steady-state (60 Hz) the secondary voltage is almost an ideal replica of the primary voltage, indicating that during steady-state this CCVT has an acceptable accuracy for most protection applications [11]. However, for any other frequency, the same fidelity is not verified, because there is a big voltage attenuation. Consequently, small primary voltage deviations, caused by disturbances in the power system may not be seen in the secondary of the transformer. Thereby, the CCVT operation during the transient may compromise the accurate measurement performed by instruments connected to the transformer, which may affect the protection algorithms performances.

B. Anti-Aliasing Filter

Anti-aliasing filters are low pass filters used before the sampling process performed by ADC to limit the signal bandpass and prevent aliasing error (overlap of signal's frequency spectrum). Nyquist theorem sets out that if a

signal has been sampled with a sampling frequency twice higher than the highest signal's frequency, this signal can be faithful recovered [1], [2]. Therefore, according to Nyquist theorem, anti-aliasing filters must eliminate components with frequencies higher than half of the ADC's sampling frequency [2].

It is common to use in protection applications a Butterworth, Chebyshev, or Bessel filter to satisfy computer relaying requirements [2]. Second and third order Butterworth filters are the most widely used before the signals are sampled by the ADC and used in numerical relays due to the fact that they do not present oscillations along the bandpass and do not promote significant angle deviations of the filtered signal [2]. In this paper, the performance of a third order Butterworth filter is evaluated in cascade with the CCVT presented in section II-A and with three ADC presented in section II-C regarding the impact on fault locators.

For the phasor estimation routine used in the analysis (see section III), the sampling rate f_s used was chosen as 960 Hz, therefore, the cut-off frequency f_c of the anti-aliasing filter must be at most a value of $f_s/2$ (480 Hz) according to the Nyquist criteria. The cut-off frequency value chosen was 380 Hz, due to be around 80% of the Nyquist frequency. The ideal and anti-aliasing filters frequency responses is shown in Fig. 4 and transfer function (described in (1)) for the evaluated filter.

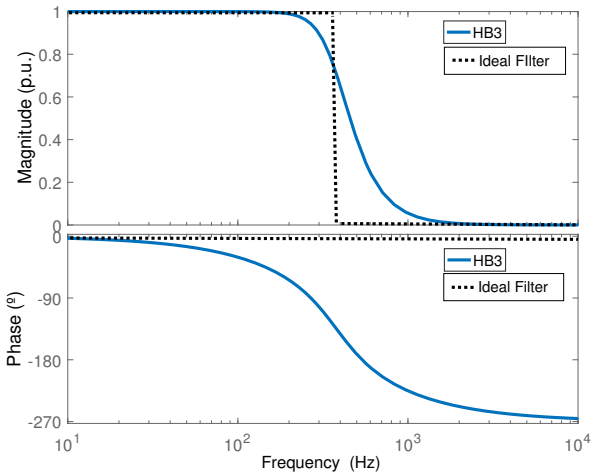

Fig. 4: Ideal and third order Butterworth filters frequency responses.

$$HB3 = \frac{1.361 \cdot 10^{10}}{s^3 + 4775s^2 + 1.14 \cdot 10^7 s + 1.361 \cdot 10^{10}}. \quad (1)$$

To represent in time domain the transient response of the modeled CCVT in cascade with the anti-aliasing filter during a fault, it is shown in Fig. 5 the primary, secondary, and filtered secondary voltage signals for a phase-to-ground fault applied at 40 km from the measurement point of a 230 kV power system. The fault simulations were performed using the system detailed in section IV with a time step of 5 μs.

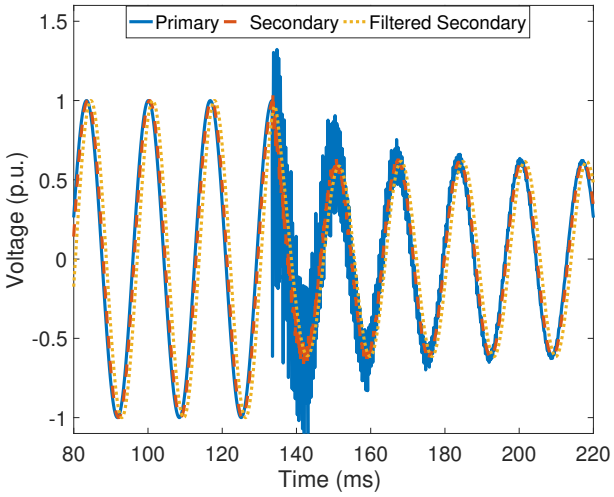

(a)

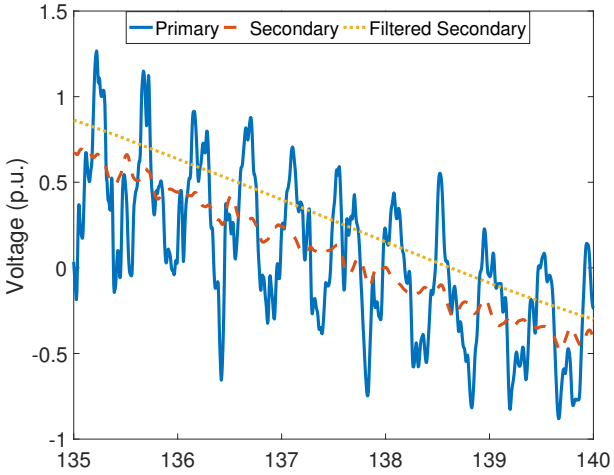

(b)

Fig. 5: CCVT primary and secondary voltages signals during a phase-to-ground fault: (a) Analyzed period (p.u.); (b) Instant of fault.

From Fig. 5, it can be observed that during the fault the secondary voltage is not a replica of the primary voltage. There is a significant attenuation on the voltage high frequency components, what can be explained by the frequency response illustrated in Fig. 3(a). Thus, such attenuation may cause undue performance of protection functions. Furthermore, it is also observed that the filter eliminates high frequency components.

C. Analog-to-Digital Converter

An ADC converts the instantaneous value of an analog voltage into a n-bit (typically 8 to 16 bits) binary number to be manipulated by microprocessors [3]. The A/D conversion involves four steps: sampling, retention, quantization and encoding. The sample-and-hold is responsible for the first two steps. Basically, this circuit samples and retains the analog signal long enough to prevent any signal variation during the quantization and encoding process, performed by the

ADC. The only degradation to be introduced during the A/D conversion is the quantization error [16]. In this paper the ADC technique chosen was the successive approximation, which is presented in [3].

According to [3], for ADC with a word size of $(b+1)$ bits and range of $-Y$ to $+Y$, the digitized value Z_{10} for a positive and negative input of X volts are defined as follows:

$$Z_{10} = INT \;\; or \;\; RON \left[\frac{X(2^b - 1)}{Y} \right], \tag{2}$$

$$Z_{10} = INT \;\; or \;\; RON \left[\frac{(2Y - |X|)2^b}{Y} \right], \tag{3}$$

where Z_{10}, INT, and RON are the integer value of base 10, the truncation and rounding operations, respectively. An output must account for the resolution (RES) of the ADC converter to provide proper output value, which is given by [3]:

$$RES = \frac{Y}{2^b - 1}. \tag{4}$$

The floating point representations for positive and negative numbers are computed, respectively, as follows:

$$PF = Z_{10} \cdot RES, \tag{5}$$

$$PF = (Z_{10} - 2^{b+1}) \cdot RES. \tag{6}$$

Here, a total of three ADC with different word sizes (8, 16, and 32 bits) were considered for the fault locators analysis.

To see, graphically, the impact of the data acquisition system on the phasor estimation algorithm chosen (see section III), in Fig. 6 are plotted the phasors using the signals from the primary, secondary, filtered secondary (But3), and the ADC (But3 AD 8b) with 8 bits output.

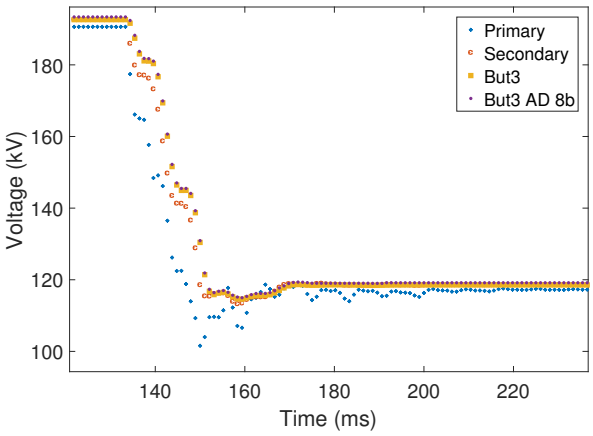

Fig. 6: Estimated phasors for the different data used as input.

From Fig. 6 it can be seen that before the fault, the phasors are similar, which does not happen during the fault. The most distorted phasors were obtained when using the data from the primary circuit, due to the fact that during a fault the transients are very severe, introducing therefore, a lot of high frequency components in the primary signals. Since the CCVT and the filter attenuate these high frequency components, the phasors estimated with these signals are less distorted. The phasors estimated using the output of the filter and the ADC are very similar because of the small quantization error introduced in the filtered signal.

III. Impedance-based Fault Locators

In this paper, the performance of two impedance-based fault locators are evaluated regarding the influence of the data acquisition system. The estimated voltage and current phasors are used in numerical relays to calculate apparent impedance between the equipment and fault location and, thus, estimate the fault location [1]. These algorithms are commonly employed to determine the location of TL faults due to their ease for implementing and provide reasonable location estimates [12], [13]. Furthermore, they can be of two types: one- and two-ended (signals captured in one or two terminals of the monitored TL) [1]. Each method possess specific input data requirements and makes certain assumptions when computing the distance to a fault, i.e., no single fault locator will yield to the best results for all different fault scenarios [14]. In this paper, the phasors quantities are computed using the Full Cycle Discrete Fourier Transform (FCDFT) [2] with a sampling rate of 960 Hz.

The FCDFT is a development of the Fourier series for a period equivalent to a fundamental cycle of a periodic sampled signal $x(m)$, considering N samples/cycle. This algorithm consists on extracting the fundamental component of a signal $x(t)$ by multiplying a cycle of samples with sine and cosine functions. This process results in one real and one imaginary components [2].

A. One-Ended Algorithm

One-ended algorithms determine the apparent impedance using voltage and current captured from only one end of the line during the fault. The main advantages of this routines are that they are straightforward to implement, yield reasonable location estimates and do not require communication channel between local and remote buses [14]. Here, the one-ended algorithm chosen was the Takagi Method (reported in [15]). This method uses the superposition principle decomposing the network during a fault into a pre-fault and "pure fault" network [14]. The fault point d is estimated by:

$$d = \frac{imag(\hat{V}_G \cdot \Delta\hat{I}_G^*)}{imag(Z_{L1} \cdot \hat{I}_G \cdot \Delta\hat{I}_G^*)}. \tag{7}$$

where $\hat{V}_G$, $\hat{I}_G$ and $\Delta\hat{I}_G$ are the voltage, current and "pure fault" current phasors captured at the monitored TL terminal, respectively, whose values vary depending on the fault type. To estimate the fault point it was used samples of three cycles after the fault detection for the "pure fault" network.

B. Two-Ended Algorithm

Two-ended algorithms use data captured at both ends (local and remote) of a monitored TL to estimate the fault point. The measurements taken from the remote bus eliminate any reactance error resulting of fault resistance

or, load current, or system non-homogeneity [14]. Unlike the one-ended techniques, two-terminal methods requires a communication channel to transfer data from one end to the other, and can be classified as synchronized (measurements from both ends are synchronized to a common time reference) or unsynchronized. Here, it is considered that the data is perfectly synchronized. The fault point d is estimated as described in (8) [14]:

$$d = \frac{\hat{V}_{G2} - \hat{V}_{H2} + Z_{L2}\hat{I}_{H2}}{(\hat{I}_{G2} + \hat{I}_{H2})Z_{L2}}, \tag{8}$$

where $\hat{V}_{G2}$ and $\hat{I}_{G2}$ are the negative-sequence voltage and current phasors at local end, respectively. $\hat{V}_{H2}$ and $\hat{I}_{H2}$ are the negative-sequence voltage and current phasors at remote end, respectively, and Z_{L2} is the negative-sequence line impedance. Although, three-phase balanced faults do not present negative-sequence, thus, equation (8) can still be used to estimate the fault point by replacing the negative-sequence components for positive-sequence components as described in (9).

$$d = \frac{\hat{V}_{G1} - \hat{V}_{H1} + Z_{L1}\hat{I}_{H1}}{(\hat{I}_{G1} + \hat{I}_{H1})Z_{L1}}. \tag{9}$$

IV. Analysis and Results

The influence of the data acquisition system on the two evaluated impedance-based fault locators was carried out through some ATP fault simulations in the power system shown in Fig. 7, which is a fictitious system with typical parameters. It was considered a 230 kV electric power system with a length of 100 km. The distance d is the point where the fault F was applied. The TL and Thévenin equivalent parameters are shown in Tables II and III, respectively [7].

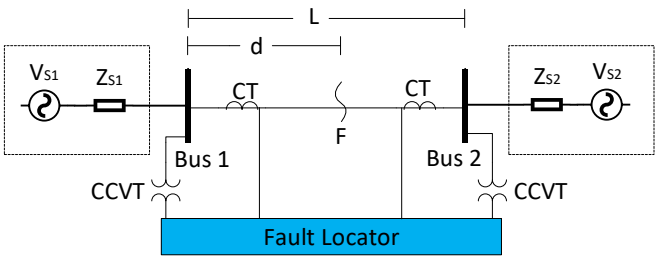

Fig. 7: 230 kV electric power system simulated in ATP.

TABLE II: Transmission line parameters.

Sequence	R(Ω/km)	X(Ω/km)	ωC(μS/km)
Positive	0,098	0,510	3,252
Zero	0.532	1.541	2.293

TABLE III: Parameters of the Thévenin equivalents.

Source	V_{th}(p.u.)	$Z_{th}(Z_{S1}, Z_{S2})$			
		$R_1(\Omega)$	$X_1(\Omega)$	$R_0(\Omega)$	$X_0(\Omega)$
S1	1.02	0.8713	25.661	1.0141	18.754
S2	0.98	0.9681	28.513	1.1268	20.838

The different simulation parameters used for each fault scenario are shown in Table IV. A total amount of 40 faults were simulated combing these different simulation variables. The ATP time step chosen for the simulations was 5 μs. After each simulation, the fault point was estimated for the considered inputs to the fault location methods: primary (reference signals), secondary, filtered secondary, and sampled voltage and current signals, and the relative errors were computed by:

$$\epsilon(\%) = \frac{|d - d'|}{L} \cdot 100, \tag{10}$$

where d and d' are the real and estimated fault point, respectively, and L is the TL length.

Since the errors were computed after each simulation, one vector was created for each technique to combine together the fault location errors for all scenarios and input data. The obtained values (μ_ϵ) and standard deviations (σ_ϵ) were calculated and are shown in Tables V and VI, for the one- and two-ended methods, respectively.

TABLE IV: Simulation parameters for the fault scenarios.

Simulation parameters	Values
Fault type	AG, AB, BCG, ABC
Fault location (km)	10, 50, 90
Inception angle (°)	0, 45, 90, 180
Fault resistance (Ω)	1, 20, 50, 100

TABLE V: Relative errors for the one-ended impedance-based fault locators for each input data.

Input Data	Relative Errors (%)	
	μ_ϵ	σ_ϵ
Primary	3.0362	5.9184
Secondary	6.0890	10.5502
Secondary+Filter	6.0410	10.5552
Secondary+Filter+ADC_8b	5.9329	10.5059
Secondary+Filter+ADC_16b	6.0406	10.5550
Secondary+Filter+ADC_32b	6.0410	10.5552

* ADC_8b, ADC_16b, and ADC_32b means ADC with a word size of 8, 16, and 32 bits, respectively.

TABLE VI: Relative errors for the two ended impedance-based fault locators for each input data.

Input Data	**Relative Errors (%)**	
	μ_ϵ	σ_ϵ
Primary	0.6871	0.7514
Secondary	0.4310	0.2976
Secondary+Filter	0.4524	0.3139
Secondary+Filter+ADC_8b	0.4498	0.2768
Secondary+Filter+ADC_16b	0.4523	0.3137
Secondary+Filter+ADC_32b	0.4524	0.3139

From the results shown in Tables V and VI, the two-terminal technique presented the best solutions (smaller errors), what was expected since there are more information available to be used in the estimations. Considering only the secondary signals used as input, good estimations were obtained comparing with the results using the reference signals, in fact, the average and standard deviation were even smaller for the two-ended algorithm. This fact can be explained analyzing Fig. 3(a), the CCVT transient response attenuates high frequency components, which improves the task of extracting the signal fundamental frequency by the phasor estimation algorithm.

Regarding the estimations computed when using the filtered secondary waveforms as input data, there was just a modest improvement, because although the anti-aliasing filter eliminates higher frequencies in the fault-induced transients, improving the phasor estimation performance, the CCVT already attenuates high frequency components of the signal, as previously stated. Concerning the estimations when using as input data the resulting signals from the three ADC, as expected, the ADC that introduced smaller errors on the filtered signals was the one with a word size of 32 bits. However, it is noticeable that the results considering all ADC were identical. Additionally, it is worth mentioning that smaller errors were observed when using the data from the ADC with a word size of 8 bits. These results make it clear that for the protection functions (impedance-based fault locators) evaluated here, converters with low-cost design are enough to obtain accurate results.

V. Conclusion

In this paper, the influence of the data acquisition system composed by one CCVT, reported in literature, one anti-aliasing filter (third order Butterworth filter) and three ADC with different designs on two impedance-based fault locators was investigated. Several ATP fault simulations were carried out varying the fault parameters as type, location, inception angle, and resistance, and after each simulation the fault point was estimated using as input data to the algorithms the signals from the primary, secondary, filtered secondary, and ADC output.

From the results, it was verified that the two-terminal technique employed is more accurate and immune to the CCVT transients than the one-ended method, what is expected due to the use of more data from the system. Since the CCVT frequency response attenuates high frequencies, there is a improvement on the phasor estimation task in extracting the fundamental frequency of the signal, which resulted in good fault point estimations. The results were slightly better when the anti-aliasing filter was used to eliminate components with frequency higher than the chosen cut-off frequency. In relation to the results when it was used the ADC, it was confirmed that the higher the word size the smaller are the error introduced, as expected. However the results were very similar for all three ADC, which indicates that even a less expensive converter as one with a word size of 8 bits meet the requirements to obtain accurate estimations.

Acknowledgment

The authors would like to thank the reviewers for their invaluable suggestions.

VI. References

[1] M. M. Saha, J. Izykowski, and E. Rosolowski, *Fault Location on Power Networks*, ser. Power Systems. London: Ed. Springer, 2010.

[2] A. G. Phadke and J. S. Thorp, *Computer Relaying for Power Systems*, 2nd ed., ser. Protective relays. England: A John Wiley and Sons Ltd, 2009.

[3] S. G. A. PEREZ, "Modeling Relays for Power System Protection Studies." Ph.D. Thesis, University of Saskatchewan, Canada, 2006.

[4] B. Naodovic, "Influence of instrument transformers on power system protection," Ph.D. dissertation, Texas AM University, 2005.

[5] D. Hou, J. Roberts, "Capacitive voltage transformer: transient overreach concerns and solutions for distance relaying," in *Electrical and Computer Engineering, 1996. Canadian Conference on*, vol. 1, May 1996, pp. 119-125 vol.1.

[6] R.L.A. Reis, W.L.A. Neves, D. Fernandes Jr., "Impact of instrument transformers and anti-aliasing filters on fault locators," *International Conference on Power Systems Transients*, Seoul, Republic of Korea, 2017.

[7] R.L.A. Reis, F.V. Lopes, W.L.A. Neves, D. Fernandes Jr., "Influence of coupling capacitor voltage transformers on travelling wave-based fault locators," *International Conference on Power Systems Transients*, Cavtat, Croatia, 2015.

[8] R.L.A. Reis, W.L.A. Neves, D. Fernandes Jr., "Influence of instrument transformers and anti-aliasing filters on the performance of fault locators," *Electric Power Systems* Research, v. 162, p. 142-149, 2018.

[9] *ATP - Alternative Transient Program*, Leuven EMTP Center, Herverlee, Belgium, 1987.

[10] *EMTP Reference Models for Transmission Line Relay Testing*, IEEE Power System Relaying Committee, 2004. [Online]. Available: http://www.pes-psrc.org

[11] E. Pajuelo, G. Ramakrishna, M. S. Sachdev, "Phasor Estimation Technique to Reduce the Impact of Coupling Capacitor Voltage Transformer Transients," University of Saskatchewan, Canada, August, 2006.

[12] IEEE Guide for Determining Fault Location on AC Transmission and Distribution Lines, IEEE Standard C37.114-2004, 2005, pp. 1-36.

[13] *Distribution Fault Location: Field Data and Analysis*, EPRI, Palo Alto, CA, USA, Tech. Rep. 1012438, 2006.

[14] S. Das, S. Santoso, A. Gaikwad, and M. Patel, "Impedance-based fault location in transmission networks: theory and application," *IEEE Access*, vol. 2, pp. 537-557, 2014.

[15] T. Takagi, Y. Yamakoshi, M. Yamaura, R. Kondow, and T. Matsushima, "Development of a new type fault locator using the one-terminal voltage and current data," *IEEE Transactions on Power Apparatus and Systems*, vol. PAS-101, no. 8, pp. 2892-2898, aug. 1982.

[16] J. PROAKIS, D. G. MANOLAKIS, *Digital Signal Processing: Principles, Algorithms, and Applications*. New Delhi: Prentice Hall, 2006.